Overview of the SuperNova/Acceleration Probe (SNAP)

G. Aldering[a], C. Akerlof[b], R. Amanullah[c], P. Astier[d], E. Barrelet[d], C. Bebek[a], L. Bergström[c], J. Bercovitz[a], G. Bernstein[e], M. Bester[f], A. Bonissent[g], C. Bower[h], W. Carithers[a], E. Commins[f], C. Day[a], S. Deustua[i], R. DiGennaro[a], A. Ealet[g], R. Ellis[j], M. Eriksson[c], A. Fruchter[k], J-F. Genat[d], G. Goldhaber[f], A. Goobar[c], D. Groom[a], S. Harris[f], P. Harvey[f], H. Heetderks[f], S. Holland[a], D. Huterer[l], A. Karcher[a], A. Kim[a], W. Kolbe[a], B. Krieger[a], R. Lafever[a], J. Lamoureux[a], M. Lampton[f], M. Levi[a], D. Levin[b], E. Linder[a], S. Loken[a], R. Malina[m], R. Massey[n], T. McKay[b], S. McKee[b], R. Miquel[a], E. Mörtsell[c], N. Mostek[h], S. Mufson[h], J. Musser[h], P. Nugent[a], H. Oluseyi[a], R. Pain[d], N. Palaio[a], D. Pankow[f], S. Perlmutter[a], R. Pratt[f], E. Prieto[m], A. Refregier[n], J. Rhodes[o], K. Robinson[a], N. Roe[a], M. Sholl[f], M. Schubnell[b], G. Smadja[p], G. Smoot[f], A. Spadafora[a], G. Tarle[b], A. Tomasch[b], H. von der Lippe[a], D. Vincent,[d] J. Walder[a], and G. Wang[a]

[a]Lawrence Berkeley National Laboratory, Berkeley CA, USA
[b]University of Michigan, Ann Arbor MI, USA
[c]University of Stockholm, Stockholm, Sweden
[d]CNRS/IN2P3/LPNHE, Paris, France
[e]University of Pennsylvania, Philadelphia PA, USA
[f]University of California, Berkeley CA, USA
[g]CNRS/IN2P3/CPPM, Marseille, France
[h]Indiana University, Bloomington IN, USA
[i]American Astronomical Society, Washington DC, USA
[j]California Institute of Technology, Pasedena CA, USA
[k]Space Telescope Science Institute, Baltimore MD, USA
[l]Case Western Reserve University, Cleveland OH, USA
[m]CNRS/INSU/LAM, Marseille, France
[n]Cambridge University, Cambridge, UK
[o]Goddard Space Flight Center, Greenbelt MD, USA
[p]CNRS/IN2P3/IPNL, Lyon, France

ABSTRACT

The SuperNova / Acceleration Probe (SNAP) is a space-based experiment to measure the expansion history of the Universe and study both its dark energy and the dark matter. The experiment is motivated by the startling discovery that the expansion of the Universe is accelerating. A 0.7 square-degree imager comprised of 36 large format fully-depleted n-type CCD's sharing a focal plane with 36 HgCdTe detectors forms the heart of SNAP, allowing discovery and lightcurve measurements simultaneously for many supernovae. The imager and a high-efficiency low-resolution integral field spectrograph are coupled to a 2-m three mirror anastigmat wide-field telescope, which will be placed in a high-earth orbit. The SNAP mission can obtain high-signal-to-noise calibrated light-curves and spectra for over 2000 Type Ia supernovae at redshifts between $z = 0.1$ and 1.7. The resulting data set can not only determine the amount of dark energy with high precision, but test the nature of the dark energy by examining its equation of state. In particular, dark energy due to a cosmological constant can be differentiated from alternatives such as "quintessence", by measuring the dark energy's equation of state to an accuracy of ± 0.05, and by studying its time dependence.

Keywords: Early universe—instrumentation: detectors—space vehicles: instruments—supernovae:general—telescopes

Correspondence: e-mail galdering@lbl.gov; telephone 510-495-2203

1. INTRODUCTION

In the past decade the study of cosmology has taken its first major steps as a precise empirical science, combining concepts and tools from astrophysics and particle physics. The most recent of these results have already brought surprises. The Universe's expansion is apparently accelerating rather than decelerating as expected solely due to gravity. This implies that the simplest model for the Universe — flat and dominated by matter — appears not to be true, and that our current fundamental physics understanding of particles, forces, and fields is likely to be incomplete.

The clearest evidence for this surprising conclusion comes from the recent supernova measurements of changes in the Universe's expansion rate that directly show the acceleration. Figure 1 shows the results of Ref. 1 (see also Ref. 2) which compare the standardized brightnesses of 42 high-redshift Type Ia supernovae (SNe Ia) ($0.18 < z < 0.83$) with 18 low-redshift SNe Ia to find that for a flat universe $\Omega_\Lambda = 0.72 \pm 0.08$ ($\Omega_M = 1 - \Omega_\Lambda$), or a deceleration parameter $q_0 = -0.58$, and constrain the combination $0.8\,\Omega_M - 0.6\,\Omega_\Lambda$ to -0.2 ± 0.1.

This evidence for a negative-pressure vacuum energy density is in remarkable concordance with combined galaxy cluster measurements,[3] which are sensitive to Ω_M, and CMB results,[4,5] which are sensitive to the curvature Ω_k (see Fig. 1). Two of these three independent measurements and standard inflation would have to be in error to make the cosmological constant (or other negative pressure dark energy) unnecessary in the cosmological models.

These measurements indicate the presence of a new, unknown energy component that can cause acceleration, hence having equation of state $w \equiv p/\rho < -1/3$. This might be the cosmological constant. Alternatively, it could be that this dark energy is due to some other primordial field for which $\rho \neq -p$, leading to different dynamical properties than a cosmological constant. The fundamental importance of a universal vacuum energy has sparked a flurry of activity in theoretical physics with several classes of models being proposed (e.g. quintessence,[6,7] Pseudo-Nambu-Goldstone Boson (PNGB) models,[8,9] cosmic defects[10,11]). Placing some constraints on possible dark energy models, Refs. 1, 12, 13 find that for a flat Universe, the data are consistent with a cosmological-constant equation of state with $0.2 \lesssim \Omega_M \lesssim 0.4$ (Fig. 2), or generally $w < -0.6$ at 95% confidence level. The cosmic string defect theory ($w = -1/3$) is already strongly disfavored.

In this paper, we attempt to formulate a definitive supernova study that will determine the values of the cosmological parameters and measure the properties and test possible models for the dark energy. In §2 we identify and discuss how to minimize systematic errors that fundamentally limit the precision with which this probe can measure cosmological parameters. A SN dataset that maximizes the resolving power of the redshift-luminosity relation under the constraint of these systematic errors is constructed in §3. We present in §4 the SuperNova / Acceleration Probe (SNAP) whose observing strategy and instrumentation suite is tailored to provide the data that satisfy both our statistical and systematic requirements.

2. CONTROL OF SYSTEMATIC UNCERTAINTIES

Type Ia SNe have already proved to be an excellent distance indicator for probing the dynamics of the Universe. However, as we move toward the era of precision cosmology, we recognize that using the SN redshift-luminosity distance relationship for measuring cosmological parameters is fundamentally limited by potential systematic errors (as are all cosmological probes).

2.1. Known Sources of Systematic Errors

Below are identified effects which any experiment that wishes to make maximal use of this technique will need to recognize and control. Following each item is the typical size of the effect on the SN brightness, along with a rough estimate of the expected *systematic* residual remaining after statistical correction for such effects with the SNAP dataset.

Malmquist Bias: A flux-limited sample preferentially detects the intrinsically brighter members of any population of sources. Directly correcting this bias would rely on knowledge of the SN Ia luminosity function, which may change with lookback time. A detection threshold fainter than peak by at least five times the intrinsic SN Ia luminosity dispersion ensures sample completeness with respect to intrinsic SN brightness, eliminating this bias ($\sim$5-10%;0%).

K-Correction and Cross-Filter Calibration: The current data set of time and lightcurve-width-dependent SN spectra needed for K-corrections is incomplete. Judicious choice of filter sets, spectral time series of representative SN Ia, and cross-wavelength relative flux calibration control this systematic ($\sim$0-10%;< 0.5%).

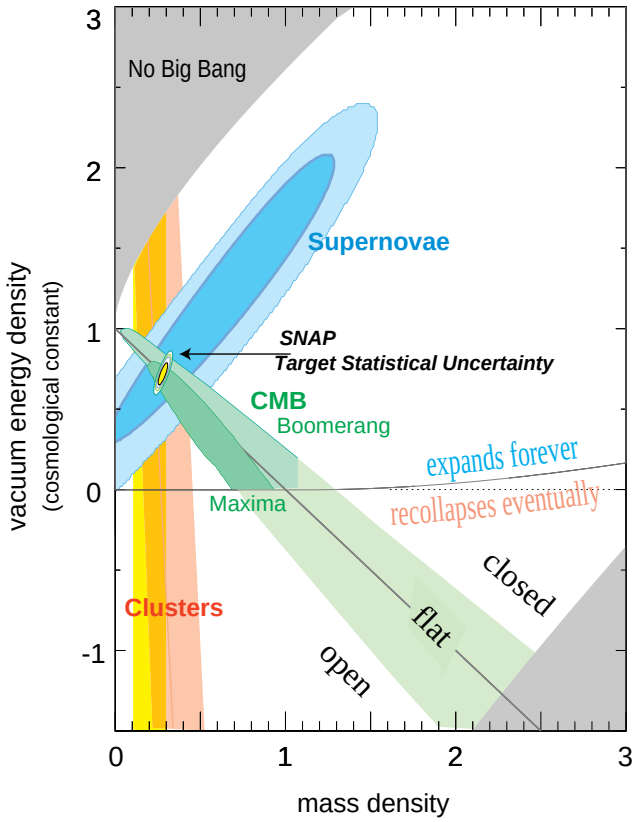

Figure 1. There is strong evidence for the existence of a cosmological vacuum energy density. Plotted are Ω_M—Ω_Λ confidence regions for current SN,[1] galaxy cluster, and CMB results. These results rule out a simple flat, [$\Omega_M = 1, \Omega_\Lambda = 0$] cosmology. Their consistent overlap is a strong indicator for dark energy. Also shown is the expected confidence region from the SNAP satellite for an $\Omega_M = 0.28$ flat Universe.

Non-SN Ia Contamination: Observed supernovae must be positively identified as SN Ia. As some Type Ib and Ic SNe have spectra and brightnesses that otherwise mimic those of SNe Ia, a spectrum covering the defining rest frame Si II 6250Å feature for every SN at maximum will provide a pure sample (∼10%;0%).

Galactic Extinction: Supernova fields can be chosen toward the low extinction Galactic poles. Future SIRTF observations will allow an improved mapping between color excesses (e.g. of Galactic halo subdwarfs in the SNAP field) and Galactic extinction by dust (∼1-10%;< 0.5%).

Gravitational Lensing by Clumped Mass: Inhomogeneities along the SN line of sight can gravitationally magnify or demagnify the SN flux. Since flux is conserved, the average of large numbers of SNe per redshift bin will give the correct average brightness. SNAP weak gravitational lensing measurements and micro-lensing studies can further help distinguish whether or not the matter is in compact objects (∼1-10%;~ 0.5%).

Extinction by Extra-Galactic "normal" Dust: Cross-wavelength flux calibrated spectra will measure any wavelength dependent absorption (∼1-20%;1%).

2.2. Possible Sources of Systematic Errors

Extinction by Gray Dust

As opposed to normal dust, gray dust is postulated to produce wavelength independent absorption in optical bands. Although physical gray dust grain models dim blue and red optical light equally, the near-IR light (∼1.2 μm) is less

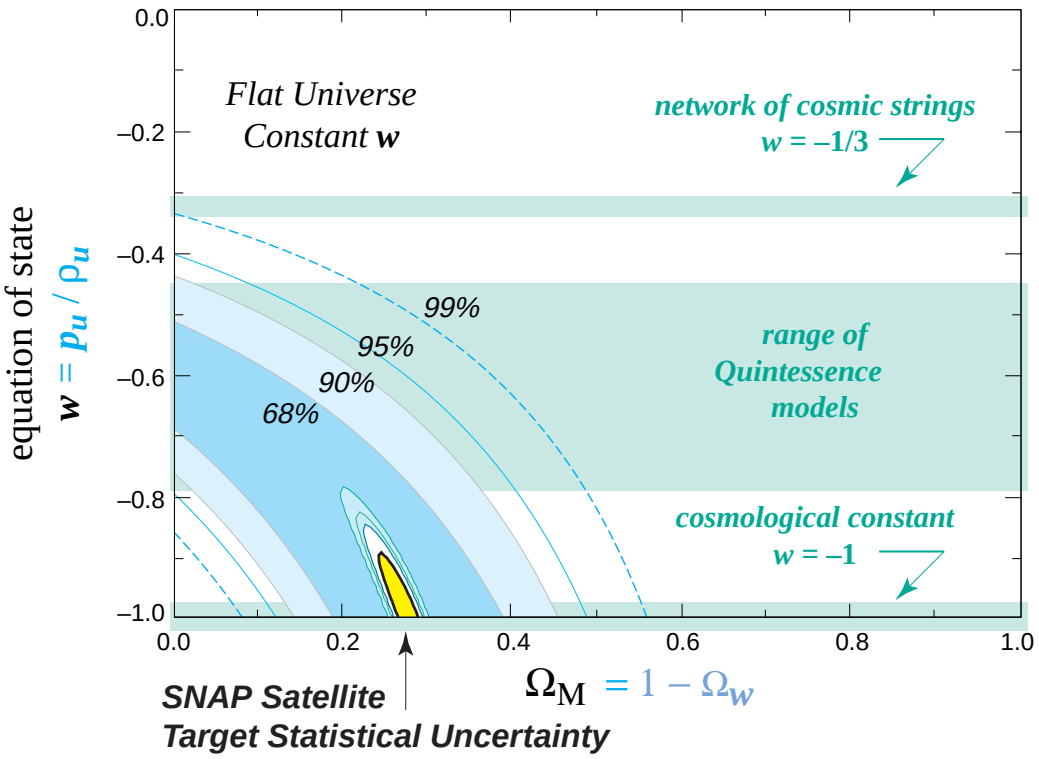

Figure 2. Best-fit 68%, 90%, 95%, and 99% confidence regions in the $\Omega_{\rm M}$–w plane for an additional energy density component, Ω_w, characterized by an equation-of-state $w = p/\rho$. (For Einstein's cosmological constant, Λ, $w = -1$.) The fit is constrained to a flat cosmology ($\Omega_{\rm M} + \Omega_w = 1$). Also shown is the expected confidence region allowed by SNAP assuming $w = -1$ and $\Omega_M = 0.28$.

affected. Cross-wavelength calibrated spectra extending to wavelength regions where "gray" dust is no longer gray will characterize the hypothetical large-grain dust's absorption properties. Armed with the extinction – color excess properties of the gray dust, broadband near-infrared colors can provide "gray" dust extinction corrections for SNe out to $z = 0.5$. Moreover, the gray dust will re-emit absorbed starlight and thus contribute to the far-infrared background. Deeper SCUBA and SIRTF observations should tighten the constraints on the amount of gray dust allowed.

Uncorrected Supernova Evolution

Supernova behavior itself may have systematic variations depending, e.g., on properties of its progenitor star or binary-star system. The distribution of these stellar properties is likely to change over time—"evolve"—in a given galaxy, and over a population of galaxies. Nearby SNe Ia drawn from a wide range of galactic environments already provide an observed evolutionary range of SNe Ia.[14, 15] The SNe differences that have been identified in these data are well calibrated by the SN Ia light curve width-luminosity relation, leaving a 10% instrinsic dispersion. As of yet, there is no evidence for systematic residuals after correction — aside from a few SNe with identified peculiarities — although observational errors would obscure such an effect. It is not clear whether any additional effects will be revealed with larger, more precise and systematic, low-redshift SNe surveys.[16]

Theoretical models can identify observables that are expected to display heterogeneity. These key features, indicative of the underlying initial conditions and physical mechanisms controlling the SN, will be measured with SNAP, allowing statistical correction for what would otherwise be a systematic error. The state of empirical understanding of these observables at the time SNAP flies will be explicitly tested by SNAP measurements. Presently, we perform Fisher matrix analyses on model spectra and lightcurves to estimate the statistical measurement requirements, and ensure that we have sensitivity to use subsamples to test for residual systematics at better than the 2% level. This approach reveals the main effects of — as well as covariance between — the following observables:

Rise time from explosion to peak: This is an indicator of opacity, fused ^{56}Ni mass and possible differences in the ^{56}Ni distribution. A 0.1 day uncertainty corresponds to a 1% brightness constraint at peak,[17] and achieving such accuracy requires discovery within ∼2 days of explosion, on average, i.e. ∼30× fainter than peak.

Plateau level 45 days past peak: The light curve plateau level that begins ∼45 days past — and more than 10× fainter than — peak is an important indicator of the C/O ratio of the progenitor star, and fused ^{56}Ni. A 5% constraint on this plateau brightness corresponds to a 1% constraint on the peak brightness.[17]

Overall light curve timescale: The "stretch factor" that parameterizes the light curve time scale is affected by almost all the aforementioned parameters since it tracks the SN Ia's lightcurve development from early to late times. It is correlated with rise time and plateau level, and it ties SNAP's controls for systematics to the controls used in the current ground-based work. A 0.5% uncertainty in the stretch factor measurement corresponds to a ∼1% uncertainty at peak.[1]

Spectral line velocities: The velocities of several spectral features throughout the UV and visible make an excellent diagnostic of the overall kinetic energy of the SNe Ia. Velocities constrained to ∼250 km s^{-1} constrain the peak luminosity ∼1%,[17] given a typical SNe Ia expansion velocity of 15,000 km s^{-1}.

UV Spectral features: The positions of various spectral features in the restframe UV are strong indicators of the metallicity of the SNe Ia. By achieving a reasonable S/N on such features SNAP will be able to constrain the metallicity of the progenitor to 0.1 dex.[18] Spectral features in the restframe optical (Ca II H&K and Si II at 6150 Å) provide additional constraints on the opacity and luminosity of the SN Ia.[19]

By measuring all of the above features for each SN we can tightly constrain the physical conditions of the explosion, making it possible to recognize subsets of SNe with matching initial conditions. The approach which SNAP makes possible is to measure each feature well enough to ensure a small luminosity range for each SNe subset categorized according to physical condition. The expected residual systematics from effects such as Malmquist bias, K-correction, etc, discussed at the beginning of this section, total ∼2%. Thus, a subset analysis based on physical conditions should group SNe to within <2% in luminosity, and this is a goal in addition to a purely statistical correction for any 2nd-parameter effects.

In addition to these features of the SNe themselves, we will also study the host galaxy of the supernova. We can measure the host galaxy luminosity, colors, morphology, and the location of the SN within the galaxy, even at redshifts z ∼1.7. Such observations are difficult or impossible from the ground.

3. SUPERNOVAE AS A PROBE OF THE DARK ENERGY

Our primary scientific objective is to use most efficiently the leverage available in the redshift-luminosity distance relationship to measure the matter and dark energy densities of the Universe with small statistical and systematic errors, and also test the properties and possible models for the dark energy. We thus determine the number of SNe we need to find, how they should be distributed in redshift, and how precisely we need to determine each one's peak brightness.

The intrinsic peak-brightness dispersion of SNe Ia after light-curve shape and extinction correction is ∼10%, so from a statistical standpoint there is no need to measure the corrected peak brightness to better than ∼10%. With such statistical accuracy, a large sample — ∼2000 SNe Ia — is required to meet the measurement goals given in Table 1. This large sample is also necessary to allow model-independent checks for any residual systematics or refined standardization parameters, since the sample will have to be subdivided in a multidimensional parameter space of redshift, lightcurve-width, host properties, etc.

The importance of using SNe Ia over the full redshift range out to $z \sim 1.7$ for measuring the cosmological parameters is demonstrated in Fig. 3 which shows the statistical uncertainty in measuring the equation of state parameter, w, as a function of maximum redshift probed in SN Ia surveys.[20] This simulation considers 2000 SNe Ia in the range $0.1 \leq z \leq z_{\max}$ measured with SNAP, along with 300 low-redshift SNe Ia from the Nearby Supernova Factory.[16] A statistical error of 15% was assigned to each SN, which includes statistical measurement error and intrinsic error. A flat universe is assumed. Two classes of models were considered, one in which w is forced to be constant with time and a second in which w varies with time according to the linear expansion $w = w_0 + w'z$. The former case is applicable to a cosmological constant or a network of topological defects, while the latter case is applicable for all other models. For these two types of models, two types of experiments were considered. The first is an idealized experiment subject only to statistical errors and free of any systematic errors. The second is a much more realistic model which assumes both statistical and systematic

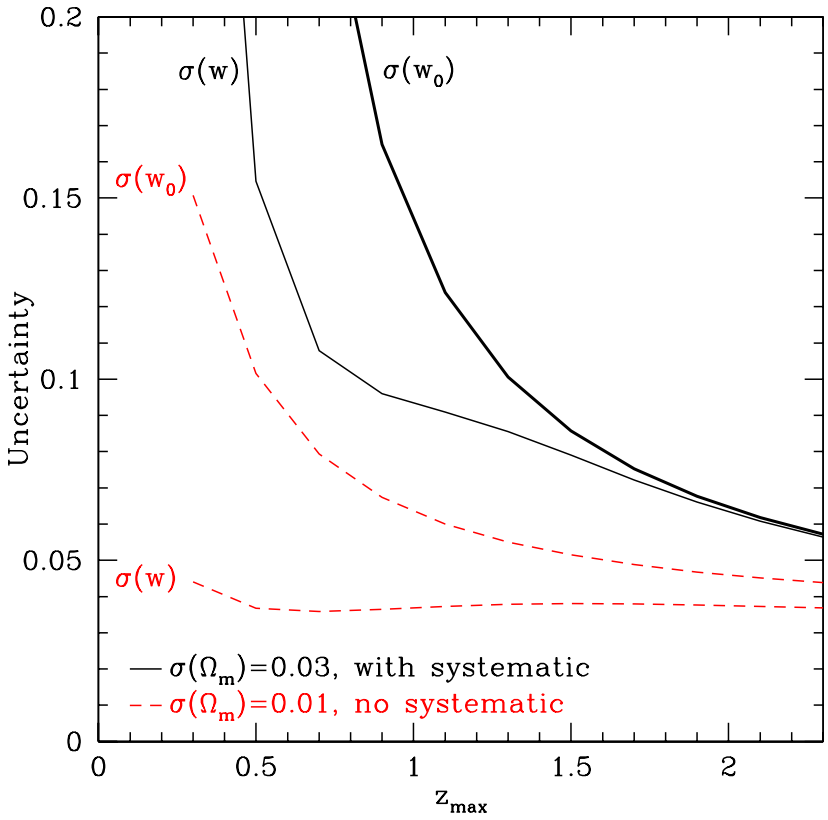

Figure 3. Accuracy in estimating the equation of state parameter, w, as a function of maximum redshift probed in SN Ia surveys.[20] The cases where w is assumed constant in time are labeled as $\sigma(w)$, while the cases where w is allowed to vary with time as $w = w_0 + w'z$ are labeled as $\sigma(w_0)$. The lower two curves assume that the experiment is free of any systematic errors, while the upper two curves are for the case where systematic errors are present at the 2% level. The top, heavy curve corresponds to the most realistic case. It is clear that even with modest systematic errors good accuracy requires probing to high redshift. In all cases a flat universe is assumed; a prior is also placed on Ω_M, with a less constrained prior of $\sigma_{\Omega_M} = 0.03$ for the cases where systematics are taken into account.

errors, with the systematic errors being very small like those SNAP can achieve. Ω_M is constrained in both cases, with a prior which itself reflects the impact of systematics, i.e., $\sigma_{\Omega_M} = 0.01$ for an ideal experiment and $\sigma_{\Omega_M} = 0.03$ for a more realistic case.

From this figure we conclude that a SNe Ia sample extending to redshifts of $z > 1$ is crucial for any realistic experiment in which there are some systematic errors remaining after all statistical corrections are applied. It is also clear that ignoring systematic errors can lead to claims which are too optimistic.

Although current data indicate that an accelerating dark energy density—perhaps the cosmological constant—has overtaken the decelerating mass density, they do not tell us the actual magnitude of either one. These two density values are two of the fundamental parameters that describe the constituents of our Universe, and determine its geometry and destiny. SNAP is designed to obtain sufficient brightness-redshift data for a large enough range of redshifts ($0.1 < z < 1.7$) that these absolute densities can each be determined to unprecedented accuracy (see Fig. 1). Taken together, the sum of these energy densities then provides a measurement of the curvature of the Universe. Assuming that the dark energy is the cosmological constant, this experiment can simultaneously determine mass density Ω_M to accuracy of 0.02, cosmological constant energy density Ω_Λ to 0.05 and curvature $\Omega_k = 1 - \Omega_M - \Omega_\Lambda$ to 0.06. The expected parameter measurement precisions for this and other cosmological scenarios are summarized in Table 1; note that these values are sensitive to the

Table 1. SNAP 1-σ statistical and systematic uncertainties in parameter determination

	σ_{Ω_M}		σ_{Ω_Λ} (or $\sigma_{\Omega_{\rm D.E.}}$)		σ_w		$\sigma_{w'}$	
	stat	sys	stat	sys	stat	sys	stat	sys
$w = -1$	0.02	0.02	0.05	< 0.01	—	—	—	—
$w = -1$, flat	—	—	0.01	0.02	—	—	—	—
$w = \text{const}$, flat	—	—	0.02	0.02	0.05	< 0.01	—	—
Ω_M, Ω_k known; $w = \text{const}$	—	—	—	—	0.02	< 0.01	—	—
Ω_M, Ω_k known; $w(z) = w_0 + w'\, z$	—	—	—	—	0.08	< 0.01	0.12	0.15

specific choice of dark energy model and parameter priors.

The SNAP experiment is one of very few that can study the dark energy directly, and test a cosmological constant against alternative dark energy candidates. Assuming a flat Universe with mass density Ω_M and a dark energy component with a non-evolving equation of state, this experiment will be able to measure the equation of state ratio w with accuracy of 0.05 (for constant w), at least a factor of five better than the best planned cosmological probes, including systematic errors.[21,22] With such a strong constraint on w we will be able to differentiate between the cosmological constant and such theoretical alternatives as topological defect models and a range of dynamical scalar-field ("quintessence") particle-physics models (see Fig. 2). Moreover, with data of such high quality one can relax the assumption of the constant equation of state, and test its variation with redshift, as predicted by many theories including supergravity and M-theory inspired models. These determinations would directly shed light on high energy field theory and physics of the early Universe.

CMB measurements from Planck will provide valuable complementarity and cross comparison with SNAP, however CMB measurements are unable to study $w(z)$. Other cosmological measurements are and will be available, but those with sensitivity to $w(z)$ still have significant systematics yet to be identified and overcome. The simultaneous fits of these measurements can improve constraints by as much as an order of magnitude — or they may not agree and upset our cosmological understanding.

4. BASELINE EXPERIMENT

To accomplish a rigorous test, discovery and study of more SNe and more distant SNe (or any probe) is by itself insufficient. As just shown, we must address each of the systematic concerns while making precise SN measurements, requiring a major leap forward in the measurement techniques. The science goals have thus driven us to the SNAP satellite experiment that we describe in this section.

4.1. Instrumentation

The baseline for the SuperNova/Acceleration Probe is comprised of a simple, dedicated combination of a 2-m telescope three-mirror-anastigmat,[23] a 0.7 square-degree optical–NIR imager and a low resolution (R$\sim$100) spectrograph sensitive in the wavelength range 0.35 – 1.7 μm. A feedback loop based on fast-readout chips on the focal plane is used to stabilize the image. A prototype of SNAP is illustrated in Fig. 4. The mirror aperture is about as small as it can be before photometry and spectroscopy at the requisite resolutions are no longer zodiacal-light-noise limited. A smaller mirror design would quickly degrade the achievable S/N of the spectroscopy measurements, and drastically reduce the number of SNe Ia followed. The three-mirror-anastigmat, illustrated in Fig. 5, achieves a corrected field 1.4 degree in diameter, and the fraction of the focal plane to populate with detectors has been chosen to obtain the follow-up photometry of multiple SNe Ia simultaneously. A smaller field would require multiple pointings of the telescope and again would greatly reduce the number of SNe Ia that could be followed. The spectrograph covers the wavelength range necessary to capture, over the entire target redshift range, the Si II 6150 Å feature that both identifies SNe Ia and provides a key measurement of the explosion physics to probe the progenitor state.

The wide field of view of the SNAP imager allows simultaneous batch discovery and photometry, and over the mission lifetime will yield $\sim$2000 SNe with the proposed accuracy. Even higher numbers of more distant, less precisely measured SNe will be available in our data set. The wide-field imager covers 0.68 square-degrees of sky. 0.34 square degrees

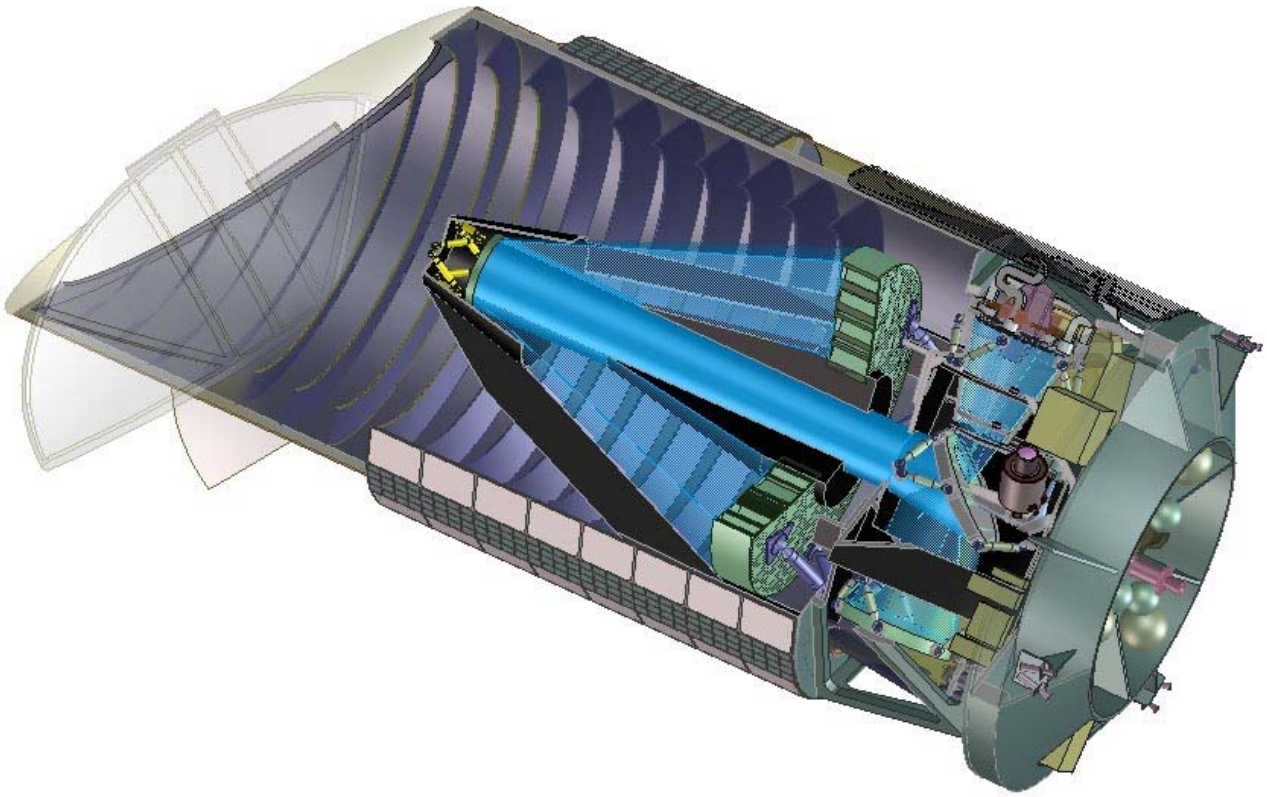

Figure 4. A cross-sectional view of the SNAP satellite. The principal assembly components are the telescope, optical bench, instruments, propulsion deck, bus, stray light baffles, thermal shielding and entrance door.

consists of a mosaic of LBNL new technology n-type high-resistivity CCD's [24–26] that have high (∼80%) quantum efficiency for wavelengths between 0.35 and 1.0 μm. Each of the 3.5k×3.5k CCD's have 10.5 μm pixels which give 0.1″ per pixel with readout noise of 4e$^-$ and dark current less than 0.002 e$^-$ pixel^{-1} sec^{-1}.[27] Extensive radiation testing shows that these CCD's will suffer little or no performance degradation over the lifetime of SNAP.[28,29] An additional 0.34 square degrees is covered by an array of 36 HgCdTe detectors [30]; we will use commercially available 2k×2k, 1.7 μm cutoff devices with 18 μm pixels, high ($\sim 60\%$) quantum efficiency, low (~ 0.1 e$^-$ pixel^{-1} sec^{-1}) dark current, and 5 e$^-$ readout noise.[31] For exposures longer than a few minutes the zodiacal light always dominates the detector noise.

Fixed filters are placed on each detector, arranged in the focal plane such that each piece of sky can be observed in each filter with a shift and stare mode of operation (Figure 6). The relative areas of each filter scale the cumulative exposure times to give limiting fluxes per unit frequency that are nearly constant from 0.35–1.7 μm. The imager will run a concurrent search and follow-up of SNe Ia over the entire redshift range $0.1 \leq z \leq 1.7$ in wavelengths between 0.35 and 1.7 μm.

The SNAP spectrograph relies on an integral field unit (IFU) to obtain an effective image of a $3'' \times 3''$ field, split into approximately $0.15''$ by $3''$ regions that are individually dispersed to obtain a flux at each position and wavelength.[32] A prism provides a high-throughput dispersive element that makes possible observations of $z = 1.7$ SNe Ia with brightness 24 magnitudes at $\lambda = 1.6$ μm (on the Vega system), with a 2-m aperture telescope. The broad SN spectral features require only low resolution ($R \sim 100$). This resolution is achieved across the visible–NIR spectrum with the prism used in single-pass for blue wavelengths and double-pass for red wavelengths. The visible detector is an LBNL CCD while the NIR detector is HgCdTe, both as described above, but with a goal of improved noise properties relative to the imager detectors. Together they provide high quantum efficiency from $0.35 - 1.7\mu$m. In operation, the IFU will allow

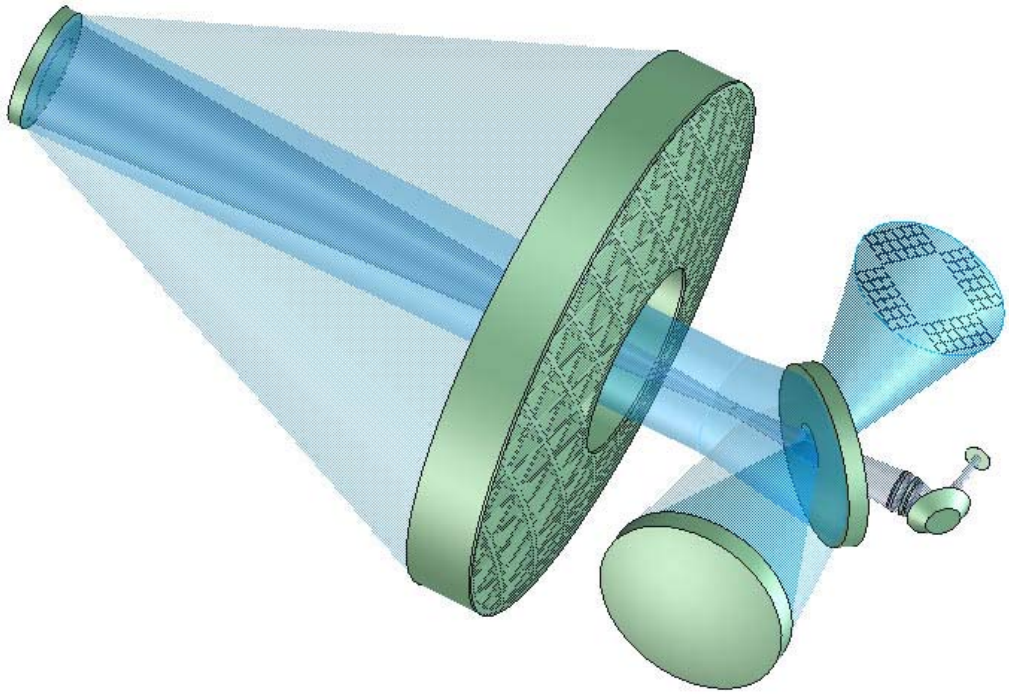

Figure 5. Side view of our baseline optical configuration, with a 2-m primary mirror, a 0.45 meter secondary mirror, a folding flat, and a 0.7 meter tertiary mirror. An optional auxiliary focus using the center of the field is possible.

simultaneous spectroscopy of a SN target and its surrounding galactic environment; the $3'' \times 3''$ field of view also removes any requirement for precise positioning of a SN target in a traditional spectrograph slit and simplifies eventual subtraction of a host galaxy spectrum. This point is particularly important for absolute flux calibration, because all of the SN light is collected with the IFU. The spectrograph is thus designed to allow use of the spectra to obtain photometry in any synthetic filter band that one chooses.

SNAP fits within a Delta-IV launch vehicle, and will be placed in high-earth orbit in order to avoid thermal loading from the Earth. Passive cooling of the focal plane is then achieved by restricting one side of the spacecraft to face the Sun, and placing a radiator in the spacecraft shadow. Passive cooling eliminates the need for cryogens, which would otherwise increase the mass and decrease the lifetime of SNAP. Orbital perigee will occur over the 11-m ground station at the Space Sciences Lab (SSL) in Berkeley, allowing downloading of the ~ 3.5 Tbits of science data generated in each 3-day orbit. Mission operations will be handled at SSL.

4.2. Observation Strategy and Baseline Data Package

This instrumentation will be used with a simple, predetermined observing strategy designed to repeatedly monitor regions of sky near the north and south ecliptic poles together covering 15 square degrees, discovering and following SNe Ia that explode in those regions. Every field will be visited at least every four days, with sufficiently long exposures that almost all SNe Ia in the SNAP survey region will be discovered within a few restframe days restframe days of explosion. (SNe at much higher redshifts on average will be found slightly later in their light curve rise times.) The periodic observation of fixed fields ensures that every SN at $z < 1.7$ will be followed as it brightens and fades.

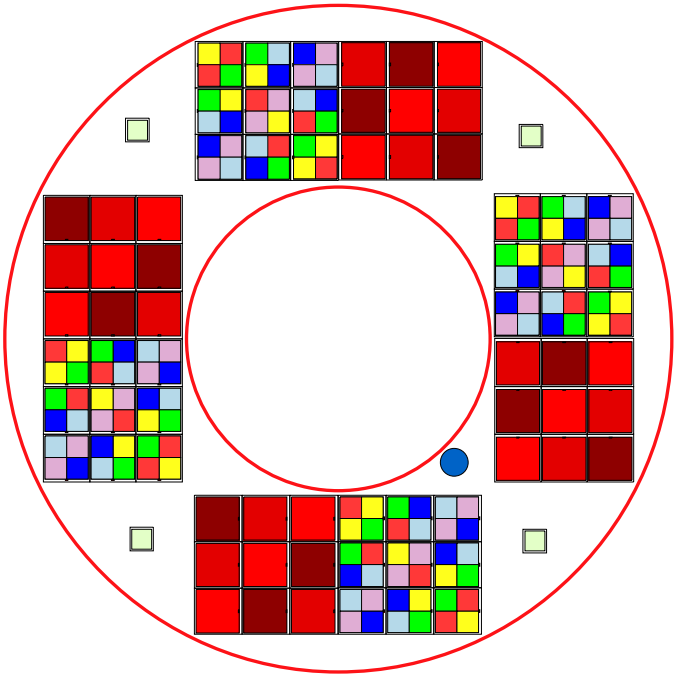

Figure 6. The SNAP mosaic camera is tiled with 36 3.5k×3.5k high-resistivity CCD's and 36 HgCdTe detectors, covering 0.7 square degrees. The dectectors are arrayed to allow step and stare sky coverage in orthogonal directions while coping with the central obscuration that is necessary in a simple three-mirror anastigmat telescope design. Each CCD is covered with four fixed filters, while each HgCdTe has one fixed filter.

This prearranged observing program will provide a uniform, standardized, calibrated dataset for each SN, allowing for the first time comprehensive comparisons across complete sets of SNe Ia. The following strategies and measurements will address, and often eliminate, the statistical and systematic uncertainties described in § 2.

- Blind, batch-processed searching.
- SNe Ia at $0.1 \leq z \leq 1.7$.
- Spectrum for every SN at maximum covering the rest frame Si II 6250 Å feature.
- Spectral time series of representative SN Ia, with cross-wavelength relative flux calibration.
- A light curve sampled at frequent, standardized intervals that extends from ∼2-80 restframe days after explosion to obtain a light-curve-width- and extinction-corrected peak rest-frame B brightness to 10%.
- Multiple color measurements in 9 bands approximating rest-frame B.
- Final reference images and spectra to enable clean subtraction of host galaxy light.

The quality of these measurements is as important as the time and wavelength coverage, so we require:

- Control over S/N for these photometry and spectroscopy measurements, to permit the targeted high statistical significance for SNe over the entire range of redshifts.
- Control over calibration for these photometry and spectroscopy measurements, with constant monitoring data collected to measure cross-instrument and cross-wavelength calibration.

Note that to date no single SN Ia has ever been observed with this complete set of measurements, either from the ground or in space, and only a handful have a dataset that is comparably thorough. With the observing strategy described here, *every one* of $\sim$2000 followed SN Ia will have this complete set of measurements.

Each systematic will either be measured, so that it can become part of the statistical error budget, or bounded. In addition the completeness of the dataset will make it possible to monitor the physical properties of each SN explosion, allowing studies of effects that have not been previously identified or proposed.

Finally, we note that SNAP will be able to make complementary measurements of the cosmological parameters using weak gravitational lensing and Type II supernovae. Moreover, the wide-field, deep, visible/NIR imaging which SNAP will produce will be an amazing resource for many other areas of study.

5. CONCLUSION

The surprising discoveries of recent years make this a fascinating new era of empirical cosmology, addressing fundamental questions. SNAP presents a unique opportunity to extend this exciting work and advance our understanding of the Universe.

ACKNOWLEDGMENTS

This work was supported by the Director, Office of Science, of the U.S. Department of Energy under contract No. DE-AC03-76SF00098.

REFERENCES

1. S. Perlmutter, G. Aldering, G. Goldhaber, R. A. Knop, P. Nugent, P. G. Castro, S. Deustua, S. Fabbro, A. Goobar, D. E. Groom, I. M. Hook, A. G. Kim, M. Y. Kim, J. C. Lee, N. J. Nunes, R. Pain, C. R. Pennypacker, R. Quimby, C. Lidman, R. S. Ellis, M. Irwin, R. G. McMahon, P. Ruiz-Lapuente, N. Walton, B. Schaefer, B. J. Boyle, A. V. Filippenko, T. Matheson, A. S. Fruchter, N. Panagia, H. J. M. Newberg, and W. J. Couch, "Measurements of Omega and Lambda from 42 High-Redshift Supernovae," *Astrophys J.* **517**, pp. 565–586, 1999.
2. A. G. Riess, A. V. Filippenko, P. Challis, A. Clocchiatti, A. Diercks, P. M. Garnavich, R. L. Gilliland, C. J. Hogan, S. Jha, R. P. Kirshner, B. Leibundgut, M. M. Phillips, D. Reiss, B. P. Schmidt, R. A. Schommer, R. C. Smith, J. Spyromilio, C. Stubbs, N. B. Suntzeff, and J. Tonry, "Observational Evidence from Supernovae for an Accelerating Universe and a Cosmological Constant," *Astron. J.* **116**, pp. 1009–1038, 1998.
3. N. A. Bahcall, J. P. Ostriker, S. Perlmutter, and P. J. Steinhardt, "The Cosmic Triangle: Revealing the State of the Universe," *Science* **284**, p. 1481, 1999.
4. A. Balbi, P. Ade, J. Bock, J. Borrill, A. Boscaleri, P. De Bernardis, P. G. Ferreira, S. Hanany, V. Hristov, A. H. Jaffe, A. T. Lee, S. Oh, E. Pascale, B. Rabii, P. L. Richards, G. F. Smoot, R. Stompor, C. D. Winant, and J. H. P. Wu, "Constraints on Cosmological Parameters from MAXIMA-1," *Astrophys. J.* **545**, pp. L1–LL4, 2000.
5. A. E. Lange, P. A. Ade, J. J. Bock, J. R. Bond, J. Borrill, A. Boscaleri, K. Coble, B. P. Crill, P. de Bernardis, P. Farese, P. Ferreira, K. Ganga, M. Giacometti, E. Hivon, V. V. Hristov, A. Iacoangeli, A. H. Jaffe, L. Martinis, S. Masi, P. D. Mauskopf, A. Melchiorri, T. Montroy, C. B. Netterfield, E. Pascale, F. Piacentini, D. Pogosyan, S. Prunet, S. Rao, G. Romeo, J. E. Ruhl, F. Scaramuzzi, and D. Sforna, "Cosmological parameters from the first results of Boomerang," *Phys. Rev. D* **63**, p. 42001, 2001.
6. R. R. Caldwell, R. Dave, and P. J. Steinhardt, "Cosmological Imprint of an Energy Component with General Equation of State," *Physical Review Letters* **80**, pp. 1582–1585, 1998.
7. I. Zlatev, L. Wang, and P. J. Steinhardt, "Quintessence, Cosmic Coincidence, and the Cosmological Constant," *Physical Review Letters* **82**, pp. 896–899, 1999.
8. J. A. Frieman, C. T. Hill, A. Stebbins, and I. Waga, "Cosmology with Ultralight Pseudo Nambu-Goldstone Bosons," *Physical Review Letters* **75**, pp. 2077–2080, 1995.
9. K. Coble, S. Dodelson, and J. A. Frieman, "Dynamical Λ models of structure formation," *Phys. Rev. D* **55**, pp. 1851–1859, 1997.
10. A. Vilenkin, "String-Dominated Universe," *Physical Review Letters* **53**, pp. 1016–1018, 1984.

11. A. Vilenkin and E. Shellard, *Cosmic Strings and other Topological Defects*, Cambridge University Press, Cambridge, U.K., 1994.
12. P. M. Garnavich, S. Jha, P. Challis, A. Clocchiatti, A. Diercks, A. V. Filippenko, R. L. Gilliland, C. J. Hogan, R. P. Kirshner, B. Leibundgut, M. M. Phillips, D. Reiss, A. G. Riess, B. P. Schmidt, R. A. Schommer, R. C. Smith, J. Spyromilio, C. Stubbs, N. B. Suntzeff, J. Tonry, and S. M. Carroll, "Supernova Limits on the Cosmic Equation of State," *Astrophys. J.* **509**, pp. 74–79, 1998.
13. S. Perlmutter, M. S. Turner, and M. White, "Constraining Dark Energy with Type Ia Supernovae and Large-Scale Structure," *Physical Review Letters* **83**, pp. 670–673, July 1999.
14. M. Hamuy, M. M. Phillips, N. B. Suntzeff, R. A. Schommer, J. Maza, and R. Aviles, "The Absolute Luminosities of the Calan/Tololo Type IA Supernovae," *Astron. J.* **112**, p. 2391, 1996.
15. M. Hamuy, S. C. Trager, P. A. Pinto, M. M. Phillips, R. A. Schommer, V. Ivanov, and N. B. Suntzeff, "A Search for Environmental Effects on Type IA Supernovae," *Astron. J.* **120**, pp. 1479–1486, 2000.
16. G. Aldering and The Nearby Supernova Factory collaboration, "An Overview of the Nearby Supernova Factory," in *Proc. SPIE Vol. 4836, Astronomical Telescopes and Instrumentation*, **4836**, 2003.
17. P. Hoeflich, J. C. Wheeler, and F. K. Thielemann, "Type IA Supernovae: Influence of the Initial Composition on the Nu cleosynthesis, Light Curves, and Spectra and Consequences for the Determination of Omega M and Lambda," *Astrophys. J.* **495**, p. 617, 1998.
18. E. J. Lentz, E. Baron, D. Branch, P. H. Hauschildt, and P. E. Nugent, "Metallicity Effects in Non-LTE Model Atmospheres of Type IA Supernovae," *Astrophys. J.* **530**, pp. 966–976, 2000.
19. P. Nugent, M. Phillips, E. Baron, D. Branch, and P. Hauschildt, "Evidence for a Spectroscopic Sequence among Type 1a Supernovae," *Astrophys. J.* **455**, p. L147, 1995.
20. E. V. Linder and D. Huterer, "Importance of SNe at $z > 1.5$ to Probe Dark Energy,"
21. J. Weller and A. Albrecht, "Opportunities for Future Supernova Studies of Cosmic Acceleration," *Physical Review Letters* **86**, pp. 1939–1942, 2001.
22. J. Weller and A. Albrecht, "Future supernovae observations as a probe of dark energy," *Phys. Rev. D* **65**, 2002.
23. M. Lampton and the SNAP Collaboration, "SNAP Telescope," in *Proc. SPIE Vol. 4854, Astronomical Telescopes and Instrumentation*, **4854**, p. 999, 2003.
24. S. E. Holland, M. Wei, K. Ji, W. E. Brown, D. K. Gilmore, R. J. Stover, D. E. Groom, M. E. Levi, N. Palaio, and S. Perlmutter, "Large Format CCD Image Sensors Fabricated on High Resistivity Silicon," in *IEEE Workshop on Charge-Coupled Devices and Advanced Image Sensors*, p. 239, 1999.
25. R. J. Stover, M. Wei, K. Ji, W. E. Brown, D. K. Gilmore, S. E. Holland, D. E. Groom, M. E. Levi, N. Palaio, and S. Perlmutter, "A 2Kx2K high resistivity CCD," in *Optical Detectors for Astronomy II: State-of-the-Art at the Turn of the Millenium*, p. 239, 2000.
26. D. E. Groom, S. E. Holland, M. E. Levi, N. P. Palaio, S. Perlmutter, R. J. Stover, and M. Wei, "Back-illuminated, fully-depleted CCD image sensors for use in optical and near-IR astronomy," *Nuclear Instruments and Methods in Physics Research A* **442**, pp. 216–222, 2000.
27. C. Bebek and the SNAP Collaboration, "SNAP Focal Plane," in *Proc. SPIE Vol. 4854, Astronomical Telescopes and Instrumentation*, **4854**, 2003.
28. C. Bebek, D. Groom, S. Holland, A. Karcher, W. Kolbe, J. Lee, M. Levi, N. Palaio, B. Turko, M. Uslenghi, M. Wagner, and G. Wang *IEEE Trans. Nucl. Sci.* .
29. C. Bebek, D. Groom, S. Holland, A. Karcher, W. Kolbe, J. Lee, M. Levi, N. Palaio, B. Turko, M. Uslenghi, M. Wagner, and G. Wang, "Radiation testing," in *Proc. SPIE Vol. 4669*, **4669**, 2003.
30. G. Tarle and the SNAP Collaboration, "SNAP NIR detectors," in *Proc. SPIE Vol. 4850, Astronomical Telescopes and Instrumentation*, **4850**, 2003.
31. J. Johnson, E. Polidan, A. Waczynski, R. Hill, G. Delo, M. Robberto, C. M. Lisse, and L. Cawley, "Dark current measurements on a state of the art near-IR HgCdTe 1024×1024 array,"
32. A. Ealet and the SNAP Collaboration, "SNAP Focal Plane," in *Proc. SPIE Vol. 4854, Astronomical Telescopes and Instrumentation*, **4854**, 2003.